Characterization and Comparison of Three Passive Air Samplers for Persistent Organic Pollutants

ARTICLE *in* ENVIRONMENTAL SCIENCE AND TECHNOLOGY · NOVEMBER 2002

Impact Factor: 5.33 · DOI: 10.1021/es020635t · Source: PubMed

2 AUTHORS:

Mahiba Shoeib
Environment Canada
59 PUBLICATIONS **3,716** CITATIONS
SEE PROFILE

Tom Harner
Environment Canada
203 PUBLICATIONS **11,372** CITATIONS
SEE PROFILE

Environ. Sci. Technol. **2002**, *36,* 4142−4151

Characterization and Comparison of Three Passive Air Samplers for Persistent Organic Pollutants

MAHIBA SHOEIB AND TOM HARNER*

Meteorological Service of Canada, Environment Canada, 4905 Dufferin Street, Toronto, Ontario M3H 5T4, Canada

The accumulation of persistent organic pollutants by three passive sampling media—semipermeable membrane devices (SPMDs), polyurethane foam (PUF) disks, and an organic-rich soil—was investigated. The media were exposed to contaminated indoor air over a period of 450 days, and concentrations in the air and in the media were monitored for individual polychlorinated biphenyl (PCB) congeners and polychlorinated naphthalene homologue groups. Uptake was initially linear and governed by the surface area of the sampler and the boundary layer air-side mass transfer coefficient (MTC). Mean values of the MTC were 0.13, 0.11, and 0.26 cm s^{-1} for SPMD, PUF, and soil, respectively. As the study progressed, equilibrium was established between ambient air and the passive sampling media for the lower molecular weight PCB congeners. This information was used to calculate passive sampler−air partition coefficients, K_{PSM-A}. These were correlated to the octanol−air partition coefficient, and the resulting regressions were used to predict K_{PSM-A} for the full suite of PCBs. Information on MTC, K_{PSM-A}, surface area, and effective thickness of each sampler was used to estimate times to equilibrium for each medium. These ranged from tens of days for the lower molecular weight congeners to tens of years for the higher molecular weight PCBs. Expressions were also developed to relate the amount of chemical accumulated by the passive sampling media to average ambient air concentrations over the integration period of the sample.

Introduction

Passive samplers are chemical accumulators that can be used to assess ambient concentrations (or fugacities) in either homogeneous or heterogeneous media into which they are deployed. They are increasingly employed in investigations of persistent organic pollutants (POPs). Examples include solid-phase microextraction (SPME) (*1*, *2*), semipermeable membrane devices (SPMDs) (*3*−*9*), and recently polymer-coated glass (POGs) (*10*, *11*). Natural and organic phases such as vegetation (*12*, *13*), soil (*14*), and even butter (*15*) have also been used to assess air burdens of POPs.

Organic media such as the ones mentioned above have a high capacity (high fugacity potential) for organic chemicals. This property allows them to accumulate airborne contaminants. The extent to which the chemicals are enriched relative to air is dependent on the passive sampler medium (PSM)−air partition coefficient, K_{PSM-A}—essentially a ratio of the analyte concentration in the PSM divided by the concentration in air when the two phases are in equilibrium. Equivalently, K_{PSM-A} is a ratio of fugacity capacities (*Z* values) in the phases of interest. Previous studies have successfully used the octanol−air partition coefficient (K_{OA}) as a surrogate for K_{PSM-A} (*5*, *16*).

In order to use passive samplers quantitatively to assess ambient air concentrations, it is necessary to know the sampling rate and K_{PSM-A}. These are determined during calibration exercises for different classes of chemicals. Qualitative interpretation of passive sampler data may also prove to be useful; for instance, for identifying chemical signatures or "fingerprints" and for assessing emission sources of POPs.

In some situations, passive samplers may be the only option. Active sampling using conventional high-volume air samplers requires pumps, sampling heads, and a source of electricity. Consequently, this type of sampling can be very costly and not always feasible, especially if several concurrent samples are required at different locations. There is an incentive therefore to further develop passive sampling technology. In this study, three organic media [SPMDs, polyurethane foam (PUF) disks, and soil] were tested and compared in terms of their functionality and versatility as passive samplers of POPs in air.

Experimental Section

Air Sampling. Three types of passive sampling media were used in this study:

U.S. Geological Survey SPMDs consisted of ∼1 g of triolein enclosed in lay-flat low-density polyethylene tubing purchased from Environmental Sampling Technologies (EST Labs, St Joseph, MO). Dimensions, 90 cm long × 2.75 cm wide; surface area, 495 cm^2; mass (triolein plus membrane), 4.41 g; volume, 8.5 cm^3; density, 0.519 g cm^{-3}; effective thickness (volume/surface area), 0.017 cm.

PUF disks are the same polyurethane foam often used for active high-volume sampling and was purchased from PacWill Environmental (Stoney Creek, ON). Dimensions, 14 cm diameter × 1.35 cm thick; surface area, 365 cm^2; mass, 4.40 g; volume, 207 cm^3; density, 0.0213 g cm^{-3}; effective thickness, 0.567 cm.

Soil was a commercial topsoil purchased from a garden center and sieved. Fraction of organic carbon, 0.095; dry soil bulk density, 0.71 g cm^{-3}; density of soil solids, 1.31 g cm^{-3}.

Ten SPMDs and PUF disks were deployed in a large laboratory of an office building (constructed ca. 1970) on four parallel rods of about 1.5 m long mounted from the ceiling. The SPMD and PUF disks were held in SPMD "spider" carriers (EST Labs, St. Joseph, MO). Five samplers were mounted on each rod with spacing of ∼30 cm between samplers. Soil was exposed in a 0.5 cm thick layer on a 40 cm diameter stainless steel tray (surface area of soil ∼1250 cm^2) mounted on one of the rods. Samples were harvested on days 0 (n = 2), 10, 29, 64 (n = 2), 170, 290 (n = 2), and 450 (n = 2 for soil). Soil samples were collected as 0.5 cm thick pie segments (∼100 cm^2), with care taken not to disturb or mix the soil remaining in the tray. The temperature in the laboratory was 22 ± 2 °C over the course of the study.

Seven active high-volume air samples (PS-1, Tisch Environmental, Cleves, OH) were collected throughout the time-course of the experiment (April 2000−June 2001). A single PUF plug (6.8 cm diameter × 4.2 cm) was used to sample the air. On two occasions (June and October 2000), the particle phase was collected by including a glass fiber filter (GFF) ahead of the PUF. The GFF was preconditioned by firing in

* Corresponding author telephone: (416)739-4837; fax: (416)739-5708; e-mail: tom.harner@ec.gc.ca.

10.1021/es020635t CCC: $22.00 Published 2002 by the Am. Chem. Soc.
Published on Web 08/31/2002

a furnace at 425 °C for 24 h. For the samples collected in August and October 2000, two PUF plugs were used in series to assess potential breakthrough of test compounds. All PUF plugs and PUF disks were precleaned by using water and then by Soxhlet extraction for 24 h using acetone and then petroleum ether. PUF plugs and disks were dried in a desiccator and stored in glass jars with Teflon-lined lids prior to and after exposure. High-volume air samples were collected over a period of 2−4 h with corresponding air volumes of 60−150 m^3.

Extraction. PUFs disks (passive samples) and front and back PUF (active samples) were individually extracted by Soxhlet in petroleum ether for 24 h. GFF were extracted by Soxhlet for 24 h using dichloromethane (DCM). Extracts were concentrated by rotary evaporation, blown down to about 1 mL with a gentle stream of nitrogen, and then solvent-exchanged into isooctane.

Extraction of soils was performed by weighing exactly ∼10−15 g into small beaker, mixing with anhydrous sodium sulfate (BDH Inc, Toronto, Canada), and then grinding using a mortar and pestle for ∼1 min until a fine, grainy consistency was achieved. The mixture was transferred to a 150-mL ceramic thimble and extracted by Soxhlet for 24 h using DCM. Thimbles were cleaned prior to use by baking for 24 h at 425 °C. Soil extracts were concentrated using a rotary evaporator and then a gentle stream of nitrogen and solvent-exchanged into isooctane. Soil moisture content was determined for each sample by weighing a portion of the sample before and after drying at 70−80 °C. Dry soil bulk density was approximated by weighing a large volume of dry soil in a 50-mL graduated cylinder. Organic carbon analysis (Desert Analytics, Tucson, AZ) was performed using a Control Equipment Corporation 440 elemental analyzer after acidification with 10% HCl to remove carbonates.

After harvesting, SPMDs were stored in the freezer in sealed aluminum containers and shipped to EST laboratory under ice for dialysis in hexane and gel permeation chromatography (GPC). Prior to dialysis, SPMDs were thoroughly brushed to remove any particle or dust stuck to the outer membrane. Extracts were concentrated to about 0.5 mL using UHP nitrogen gas, filtered through sodium sulfate, and quantitatively transferred to vials for GPC cleanup using DCM. Sample extracts were solvent-exchanged into hexane, then quantitatively transferred into ampules, and shipped back to our laboratory for further cleanup, fractionation, and quantification.

Sample Analysis. Extracts from all active and passive sampling media were fractionated on silicic acid−alumina column to separate PCBs from PAHs and polar compounds. The column consisted of 3 g of silicic acid (deactivated with 3% water) (Mallinckrodt Baker, Paris, KY) overlaid with 2 g of neutral alumina (deactivated with 6% water) (EM Science Inc. Glbbstown, NJ), and topped with 1 cm of anhydrous sodium sulfate. The column was prewashed with 30 mL of dichloromethane and then 30 mL of petroleum ether. The sample was eluted with 30 mL of petroleum ether (fraction 1, containing PCBs and PCNs) and then with 30 mL of DCM (fraction 2, containing PAHs, OC pesticides, and other polar compounds). Fractions were blown down to about 1 mL under a gentle stream of UHP nitrogen and solvent-exchanged into isooctane.

PCB congeners (2-Cl to 10-Cl) were determined using a Hewlett-Packard 5890 gas chromatograph (GC) equipped with split/splitless injector and an electron capture detector (ECD). Injector and detector temperatures were kept at 250 and 300 °C, respectively. A 60-m DB-5 column (J&W Scientific) with 0.25 mm i.d. and 0.25 μm film thickness was operated with hydrogen carrier gas. The GC oven temperature program was as follows: initial at 90 °C hold for 0.5 min, 15 °C min^{-1} to 160 °C, then 2 °C min^{-1} to 260 °C, hold for 10 min. Mirex (U.S. Environmental Protection Agency, Research Triangle Park, NC) was used as the internal standard to correct for volume difference.

TABLE 1. Mean Percent Recovery of ^{13}C PCB Surrogate Standards for Active and Passive Air Samples[a]

compd	high-volume	SPMDs	PUFs	soils
^{13}C PCB 81	81.7 (8.5)	87.8 (7.5)	88.0 (8.9)	81.8 (16)
^{13}C PCB 77	80.1 (15)	95.2 (21)	110 (24)	85.4 (19)
^{13}C PCB 105	90.8 (11)	87.9 (14)	99.9 (12)	88.4 (18)
^{13}C PCB 126	89.7 (7.2)	79.7 (11)	87.8 (14)	61.8 (6.7)

[a] SD in parentheses.

Coplanar PCBs (non-ortho congeners 77, 81, and 126 and mono-ortho congeners 105, 114, 118, and 156) were determined by gas chromatography−negative ion mass spectrometry (GC−NIMS) on a Hewlett-Packard 6890 GC-5973 mass selective detector (MSD) (all PCB standards were purchased from AccuStandard Inc, New Haven, CT). GC conditions were identical to those used for GC−ECD analysis. Methane was used as reagent gas with a flow of 2.2 mL min^{-1}. Transfer line, ion source, and quadrupole temperatures were kept at 275, 150, and 106 °C, respectively. The instrument was operated in selective ion mode (SIM) with target/qualifier ions 292/290 for tetra-PCBs, 326/328/324 for penta-PCBs and 360/362 for hexa-PCBs. Surrogate standards containing ^{13}C PCBs 77, 81, 105, and 126 (purchased from CIL, Andover, MA) were also determined using GC−NIMS with target/qualifier ions 302/304 for ^{13}C PCBs 77 and 81 and ions 336/338 for ^{13}C PCBs 105 and 126. PCNs were also determined in SIM mode with target/qualifier ions 232/230 for tri-, 266/264 for tetra-, 300/298 for penta-, 334/332 for hexa-, and 368/366 for heptachloropolychlorinated naphthalene. Quantification of PCNs was based on assigned mass contributions in Halowax1014 (U.S. EPA, Research Triangle Park, NC) as presented in Harner and Bidleman (*17*).

Quality Assurance/Quality Control. Surrogate recoveries were determined for all samples by spiking with a mixture of ^{13}C PCBs 77, 81, 105, and 126 (400 pg of each) prior to extraction (PUF disks and soil) or dialysis (SPMDs). Surrogate amounts were similar to detected quantities of native PCBs in samples. Results (Table 1) show good recoveries that range from 62% to 110%. SD values were less than 20% in more than 85% of the analyses. Recovery factors were not applied to any of the data. Previous air sampling studies in our laboratory using the same methodology have established good recoveries for the target chemicals investigated here. For instance, recoveries of PCBs were 80−120% (*18*). Duplicate blanks performed on all media were generally low and were included as the time zero value for the uptake study. Soil used in the study was obtained from an outdoor agricultural site and thus had a low level of PCB and PCN contamination resulting from extended exposure to outdoor air. However, these initial concentrations were low as compared to high levels observed during this study that resulted from exposure to the more highly contaminated indoor air.

To check for reproducibility, duplicate samples were taken for SPMD and PUF at day 0, 64, and 290, and an additional duplicate sample for soil was takem at day 450. Variability of the duplicates was in the range of 5−20% and could mostly be attributed to the inherent variability in the analytical methodology.

Quantification was done using a six point calibration curve for GC−ECD analysis of PCBs and GC−NIMS analysis of coplanar PCBs and PCNs. Thirty-seven PCB congeners were analyzed using GC−ECD. To facilitate the presentation of the data in this paper, tabulated results are only shown for selected congeners—the ICES (International Council for the

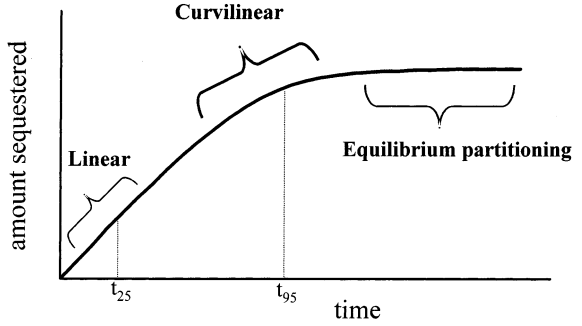

FIGURE 1. Illustrative profile for passive samplers showing three phases of uptake. Time to establish 25% and 95% of the equilibrium concentrations are also shown (t_{25} and t_{95}, respectively).

Exploration of the Sea) congeners (i.e., PCB 28, 52, 101, 137/138, 153, and 180) and additional congeners PCB 44, 99, and 128. These congeners represent nine of the more abundant 3-Cl to 7-Cl peaks in the PCB ECD profile. GC−NIMS results are reported for additional PCBs—non-ortho-PCBs 77, 81, and 126 and mono-ortho-PCBs 105, 114, 118, and 156. GC−NIMS results of PCN homologue groups (3-Cl to 7-Cl) are also reported.

Theory of Passive Air Samplers. The simplest way to model the accumulation of chemical by a passive sampling medium (PSM) is to consider it to be a uniform, porous compartment into which chemical can penetrate and/or dissolve. In this case, the mass transfer across the PSM−air interface is simply the addition of resistances in the air boundary layer and in the PSM. This is the Whitman two-film approach (*19*) where the overall mass transfer coefficient (MTC), k, can be deduced from the individual mass transfer coefficients:

$$1/k = 1/k_A + 1/(k_{PSM}K_{PSM-A}) \quad (1)$$

where k_A and k_{PSM} are the air-side and PSM-side MTCs, and K_{PSM-A} is the PSM−air partition coefficient (no dimensions). For nonpolar organic chemicals K_{PSM-A} is likely to be similar in magnitude to the octanol−air partition coefficient, K_{OA}. Thus for chemicals such as PCBs and PCNs that have large values of K_{OA} (i.e., $K_{OA} > 10^7$), the term $1/(k_{PSM}K_{PSM-A})$ is insignificant (even when k_{PSM} is simialr to k_A), and mass transfer to the passive sampler is air-side controlled, i.e., k is approximately equal to k_A.

The accumulation of chemical by the sampler is then equivalent to the rate of uptake minus the rate of loss and can be described by

$$V_{PSM}(dC_{PSM}/dt) = k_A A_{PSM}(C_A - C_{PSM}/K_{PSM-A}) \quad (2)$$

where V_{PSM} is the volume of the passive sampling medium (cm^3); C_{PSM} and C_A are concentrations (ng m^{-3}) in the PSM and air, respectively; and A_{PSM} is the planar area of the exposed portion of the passive sampler (cm^2). In this case k_A has units of cm s^{-1}.

A schematic of the uptake described by eq 2 is shown in Figure 1. Initially, when the term C_{PSM}/K_{PSM-A} is small (because C_{PSM} is minimal), uptake is linear and a function of k_A, A_{PSM}, and C_A. Ideally, these are the conditions under which the passive sampler will function when deployed in the field. Under these conditions the mass (M, ng) of analyte sequestered by the PSM can be described by

$$M = k_A A_{PSM} C_A \Delta t = b\Delta t \quad (3)$$

where Δt is the integration period of the sample in seconds.

A plot of the amount of chemical sequestered by the PSM versus time (i.e., eq 3) will have an initial slope, b, equal to $k_A A_{PSM} C_A$, i.e., the mass sampling rate in ng s^{-1}. The term $k_A A_{PSM}$ has units of cm^3 s^{-1} and represents the passive air sampling rate, R, where $R = b/C_A$. This is a very useful value because it provides a sense of how much air is sampled by the PSM. The value R can be further manipulated by dividing by the exposed area of the PSM to obtain the air-side mass transfer coefficient, k_A, (i.e., $k_A = b/(A_{PSM}C_A) = R/A_{PSM}$), which can also be viewed as a dry gaseous deposition velocity.

As chemical builds up in the PSM, the term C_{PSM}/K_{PSM-A} in eq 2 becomes more important; uptake is reduced, and the graph becomes curvilinear. Finally when C_{PSM} establishes its equilibrium (equal fugacity) value such that $C_{PSM}/K_{PSM-A} = C_A$, there is no net uptake and C_{PSM} becomes constant.

Equation 2 can be solved analytically to provide a more exact description of the uptake profile:

$$C_{PSM} = K_{PSM-A}C_A(1 - \exp - [(A_{PSM})/(V_{PSM})(k_A/K_{PSM-A})]t) \quad (4)$$

This is a first-order rate equation of the form $C = C_0 \exp(-k_U t)$ or equivalently $\ln(C/C_0) = -k_U t$, where the uptake constant k_U (units of time^{-1}) is calculated as

$$k_U = (A_{PSM})/(V_{PSM})(k_A/K_{PSM-A}) \text{ or } k_U = 1/\delta_{FILM}(k_A/K_{PSM-A}) \quad (5)$$

where $\delta_{FILM} = V_{PSM}/A_{PSM}$ is the "effective" thickness. Thus the time to 95% of equilibrium, $t_{95} = \ln(0.05)/k_U = \sim 3/k_U$ (*10*). We also arbitrarily define the upper bounds of the linear uptake phase (i.e., when uptake becomes curvilinear) as t_{25}, i.e., time when the PSM has accumulated 25% of the equilibrium value. In this case $t_{25} = \ln(0.75)/k_U = 0.29/k_U$. Equation 4 can also be rearranged to determine the average ambient air concentration C_A if C_{PSM} is measured and k_A and K_{PSM-A} are known.

It is important to note that this analysis considers only the gas-phase transfer of contaminants. It is also possible for particle-associated contaminants to become scavenged by the PSM and incorporated into the total amount of chemical sequestered. However, as noted later, this was less of a concern during this study because indoor particulate levels were low. Warmer indoor temperatures also change the physical chemistry of the pollutants, reducing the proportion on particles. In outdoor air, however, TSP (total suspended particulate) values are higher and the contribution from particle impaction may become important for compounds with $K_{OA} > 10^{10}$ that begin to partition appreciably onto particles. This effect will increase with colder temperatures since K_{OA} increases with decreasing temperature and more chemical will be associated with particles. The particle-scavenging effect can be minimized by housing the PSM in an exposure chamber. This will also protect the sampler from precipitation and sunlight and diminish the effect of wind speed on uptake rate (as the air-side MTC is sensitive to wind).

Results and Discussion

Active Air Samples. Table 2 lists the average vapor-phase concentrations of PCBs and the sum of tri- to hexa-PCN homologues for seven high-volume air samples collected throughout the 450-day time-course of the study (April, May, June, August, and October 2000; January and June 2001). Levels of PCBs were high (mean ∑PCB = 20.9 ng m^{-3})—approximately 50−100 times higher than outdoor ambient air. Levels of gas-phase PCBs and PCNs remained relatively constant throughout the study period except for the August 2000 and June 2001 samples where ∑PCB spiked to 42 and 68 ng m^{-3}, respectively. This variability may be associated with building ventilation rates that vary according to season and to daily fluctuations in outdoor temperature. Indoor air

TABLE 2. Concentrations of PCBs and PCNs in Laboratory Air As Determined by Conventional High-Volume Air Sampling ($n = 6$) over the Period April 2000−June 2001

compd	no. of Cl	mean (pg m^{-3})	minimum (pg m^{-3})	maximum (pg m^{-3})
		Multi-ortho-PCBs		
PCB 28	3	1720 ± 550	1010	2360
PCB 44	4	1080 ± 930	436	2940
PCB 52	4	1550 ± 825	684	2690
PCB 99	5	160 ± 134	65	428
PCB 101	5	490 ± 264	249	987
PCB 128	6	4 ± 2	2	9
PCB 153	6	80 ± 58	41	194
PCB 137/138	6	50 ± 21	31	77
PCB 180	7	32 ± 33	5	97
		Non-ortho- and Mono-ortho-PCBs		
PCB 77	4	10.4 ± 1.5	8.71	14.3
PCB 81	4	2.07 ± 0.8	ND	3.07
PCB 105	5	38.2 ± 9.9	32.2	49.6
PCB 114	5	3.45 ± 0.6	2.43	4.32
PCB 118	5	137 ± 25	98.2	174
PCB 126	6	0.13 ± 0.12	ND	0.42
PCB 156	6	2.73 ± 0.6	1.67	3.66
		∑PCN Homologues		
tri-PCN	3	27.5 ± 7	16.3	32.5
tetra-PCN	4	14.7 ± 2.9	11.6	17.8
penta-PCN	5	1.43 ± 0.2	1.16	1.75
hexa-PCN	6	0.20 ± 0.01	0.17	0.27

temperature may also play a role, but in this study it remained constant at ~23 °C.

The particulate-bound PCBs were evaluated in the laboratory air for two samples (June and October 2000) by including a GFF ahead of the PUF plug. Levels of PCBs and PCNs were below the detection limit. When two-thirds of the instrumental detection limit was used for the undetected congeners, particle-bound chemical represented less than 5% of the vapor-phase value. The low level of particle-associated PCBs and PCNs was expected and can be attributed to low levels of suspended particulate matter and the warm ambient temperature (23 °C) that favored gas-phase partitioning.

The breakthrough of vapor-phase PCBs through PUF was tested by including a backup PUF plug during two of the air samples (August and October 2000). Breakthrough in both samples was less then 7% for lighter PCBs (PCB 8 and 18), 1.3% and 1.8% for PCB 28, and less than 1% for tetra-PCBs and higher homologues.

SPMD. As discussed earlier, air sampling rates (R) for the SPMD can be determined from the slope (b) of the linear uptake curve (i.e., plot of amount accumulated vs time) as b/C_A. When days are used instead of seconds, R' has units of m^3 d^{-1}. Values of R' and surface area-based sampling rates (per dm^2) are listed in Table 3 for PCBs and PCNs. For the chemicals with lower K_{OA}, it was necessary to restrict the calculation to the linear portion of the uptake curve as noted in Table 3.

In Figure 2a,b, the uptake profiles for PCB 28 and 52 are expressed as an equivalent volume of air sampled (by dividing the amount of chemical sequestered at each interval by the measured mean air concentrations). PCB 28 is a good example of a chemical that experiences all three phases of uptake—linear uptake, curvilinear uptake, and equilibrium or plateau phase—illustrated in Figure 1. Equilibrium for PCB 28 is reached after only ~50−75 days when approximately 250−300 m^3 of air has been sampled. As described in eq 4, the time to equilibrium is dependent on K_{PSM-A} (or K_{OA}). For this reason, PCB 52, which has a K_{OA} value that is ~0.3 log unit (~factor of 2) larger than PCB 28 (Table 4), plateaus later (~200−400 days) after approximately 500 m^3 of air has been sampled. For chemicals with K_{OA} values greater than about 10^9 (e.g., PCB 101 and 137/138 in Figure 3a,b) uptake was linear over the entire 450-day integration period.

Air sampling rates (Table 3) for the SPMD were similar for PCBs and PCNs and usually in the range of 3−5 m^3 d^{-1} with only a few outliers. In assessing accuracy, we note that the

TABLE 3. Sampling Rates[a] Expressed on a Sampler Basis (R') and Normalized to Surface Area for Multi-ortho-, Non-ortho-, and Mono-ortho-PCBs and the Sum of Homologue Groups of PCNs for Different Sampling Media[b]

	m^3 d^{-1} or m^3 d^{-1} (g of soil)$^{-1}$ (r^2)			m^3 d^{-1} dm^{-2}		
compd	SPMD	PUF	soil	SPMD	PUF	soil
			Multi-ortho-PCBs			
PCB 28	3.8[c] (0.98)	2.8[c] (0.99)	0.03[d] (0.97)	0.77	0.83	1.1
PCB 44	3.5[c] (0.97)	2.4[c] (0.94)	0.023[d] (0.94)	0.66	0.78	0.81
PCB 52	3.9[c] (0.97)	2.4[c] (0.94)	0.040[d] (0.92)	0.66	0.86	1.4
PCB 99	3.3 (0.90)	2.2 (0.90)	0.032 (0.95)	0.61	0.74	1.1
PCB 101	3.4 (0.90)	2.0 (0.98)	0.040 (0.98)	0.53	0.75	1.4
PCB 128	5.2 (0.89)	4.2 (0.94)	0.074 (0.74)	1.2	1.2	2.6
PCB 137/138	5.4 (0.89)	3.8 (0.89)	0.071 (0.82)	1.1	1.2	2.5
PCB 153	4.1 (0.91)	3.8 (0.75)	0.039 (0.81)	1.0	0.92	1.4
PCB 180	7.9 (0.84)	8.3 (0.92)	0.17 (0.94)	1.6	1.7	5.9
			Non-ortho- and Mono-ortho-PCBs			
PCB 77	3.5 (0.97)	2.6 (0.96)	0.048 (0.95)	0.73	0.77	1.7
PCB 81	3.7 (0.93)	2.6 (0.95)	0.041 (0.99)	0.72	0.82	1.4
PCB 105	4.0 (0.95)	2.8 (0.95)	0.053 (0.90)	0.77	0.90	1.9
PCB 114	4.2 (0.97)	2.7 (0.96)	0.045 (0.95)	0.74	0.92	1.6
PCB 118	4.3 (0.96)	2.8 (0.96)	0.044 (0.95)	0.79	0.96	1.5
PCB 126	9.9 (0.97)	6.4 (0.97)	0.13 (0.90)	1.8	2.2	4.6
PCB 156	4.9 (0.98)	3.1 (0.96)	0.056 (0.83)	0.87	1.1	2.0
			∑PCN Homologues			
tri-PCN	na[e]	3.5[c] (0.98)	0.007 (0.63)	0.96	0.21	0.25
tetra-PCN	3.0[c] (0.99)	3.8[c] (0.97)	0.03 (0.89)	1.0	0.67	1.1
penta-PCN	3.2 (0.91)	1.8 (0.87)	0.06 (0.78)	0.49	0.71	2.1
hexa-PCN	5.1 (0.95)	2.8 (0.88)	0.11 (0.83)	0.77	1.1	3.9

[a] Sampling rates were determined from the linear portion of the plot of C_{PSM}/C_{AIR} vs time (C_{AIR} from Table 2) (cf. eq 3 and Figures 2 and 3). [b] Note: 1 dm^2 = 100 cm^2. [c] Calculation restricted to first 65 days. [d] Calculation restricted to first 275 days. [e] na, not available.

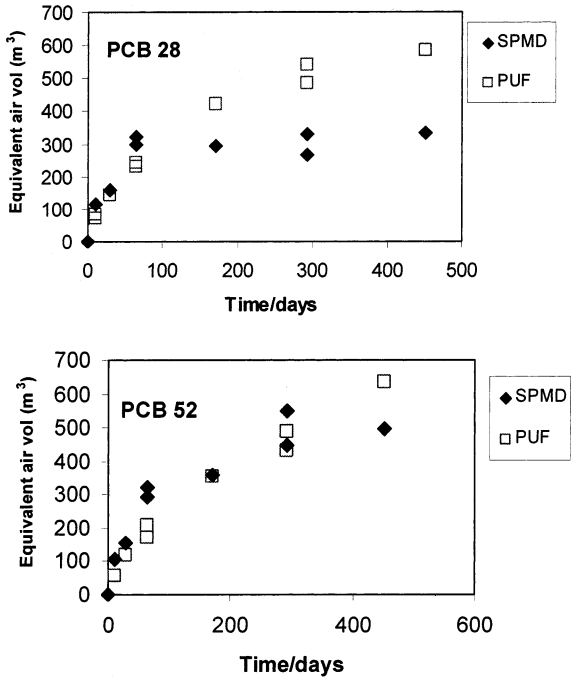

FIGURE 2. Sampling profiles for SPMD and PUF disk samplers for (a) PCB 28 and (b) PCB 52. Equivalent air volumes were calculated as C_{PSM}/C_{AIR} (C_{AIR} from Table 2) for each time interval.

TABLE 4. Estimated Equilibrium Soil Concentrations for PCBs (Calculated Using Eqs 7 and 8) As Compared with Measured Amounts at End of Uptake Study

compd	log K_{OA}[a]	log K_{SA}[b]	estd soil concn at equilibrium (ng g^{-1})[c]	sequestered amt after 450 day (ng g^{-1})	equilibrium value (%)
Multi-ortho-PCBs					
PCB 28	8.12	7.01	5.8	11	200
PCB 44	8.61	7.50	11	6.9	61
PCB 52	8.43	7.32	11	15	140
PCB 99	9.24	8.13	7.0	2.5	35
PCB 101	9.19	8.08	19	8.6	45
PCB 128	10.4	9.25	2.3	0.22	9.4
PCB137/138	10.1	9.03	18	1.5	8.4
PCB 153	9.91	8.80	17	1.3	7.7
PCB 180	10.7	9.58	40	2.4	5.9
Non-ortho- and Mono-ortho-PCBs					
PCB 77	9.75	8.64	1.5	0.25	17
PCB 81	9.67	8.56	0.24	0.04	15
PCB 105	10.2	9.06	14	1.0	7.2
PCB 114	10.0	8.93	0.84	0.07	8.3
PCB 118	9.96	8.85	32	2.9	9.1
PCB 126	10.4	9.31	0.67	0.009	1.3
PCB 156	10.8	9.64	4.3	0.08	1.9

[a] Log K_{OA} values at 23 °C for PCBs were calculated from regressions of measured K_{OA} values by Harner and Bidleman (*25*) against reported relative retention times (RRT) by Harju et al. (*26*). Separate regressions were performed for Group 1 PCBs (all congeners with IUPAC numbers lower than PCB 77 plus multi-ortho congeners higher than PCB 77) and Group 2 (PCB 77 and all other higher non-ortho- and mono-ortho-PCBs). The resulting regression had the form $\log K_{OA} = A + B(RRT)$. The above regressions were performed at several temperatures and regression coefficients (A and B values) were regressed against $1/T$ to provide temperature-dependent K_{OA} estimates with regression taking the following forms: Group 1, $A = -2.0296 + 1310.7/T$ and $B = -5.5305 + 5879.8/T$; Group 2, $A = 20.478 - 5194/T$ and $B = -49.35 + 18678/T$. [b] Using eq 7 where $\rho_{SOIL} = 1.31$g cm^{-3} and $f_{OC} = 0.095$. [c] Using eq 8 and average air concentrations (C_A) listed in Table 2.

arithmetic mean air concentrations used in the calculation of the sampling rates were generally within a factor of 2 of minimum and maximum concentrations. Thus as a worst

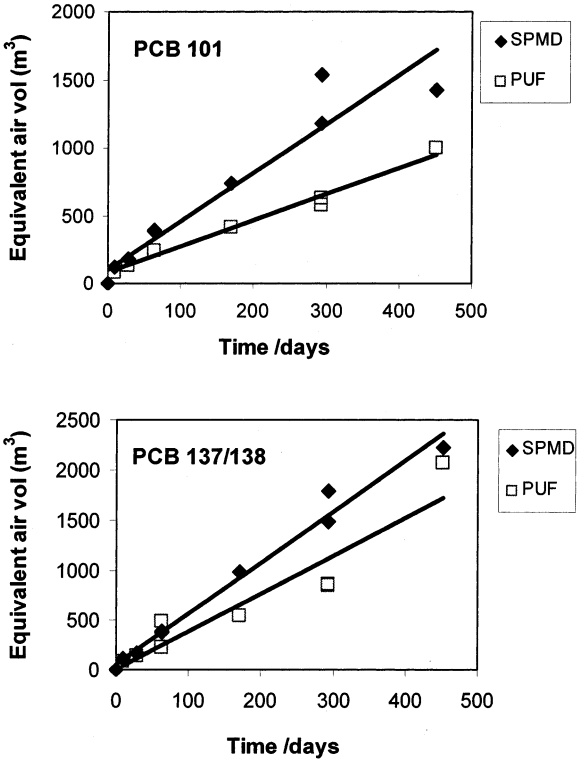

FIGURE 3. Sampling profiles for SPMD and PUF disk samplers for (a) PCB 101 and (b) PCB 137/138.

case scenario, this same factor of confidence may be applied to the sampling rates listed in Table 3.

On a surface area basis, SPMDs sampled about 1 m^3 of air d^{-1} for every dm^2 (100 cm^2) of surface area. The consistency of SPMD air sampling rates over a large range of K_{OA} (~2.5 orders of magnitude) suggests linear uptake was in fact air-side controlled and dependent upon K_{PSM-A}. Because the passive samplers were deployed in relatively still air, the air-side MTC, k_A, is likely to be similar to the chemical's molecular diffusivity in air (D_a) (cm^2 s^{-1}). (Note: On the basis of the dimensions of the room and an approximate ventilation rate of 0.3 m^3 min^{-1}, the resulting effective air velocity in the room is <0.001 cm s^{-1}, which is smaller than typical diffusivity values for these chemicals.)

Molecular diffusivity in air is a weak function of the chemicals' molar volume (V), molecular mass (m), and temperature (T), as indicated in eq 6 taken from Schwarzenbach et al. (*20*):

$$D_a = \{10^{-3}T^{1.75}[(1/m_{air}) + (1/m)]^{1/2}\}/P[V_{air}{}^{1/3} + V^{1/3}]^2 \quad (6)$$

where T is absolute temperature (K), m_{air} is the average molecular mass of air (28.97 g mol^{-1}), m is the molecular mass of the chemical (g mol^{-1}), P is gas-phase pressure (atm), V_{air} is the average molar volume of the gases in air (~20.1 cm^3 mol^{-1}), and V is the molar volume of the chemical of interest (cm^3 mol^{-1}). Thus over a 20 °C temperature range (e.g., 0−20 °C) the diffusivity will increase by only a small factor of $(293/273)^{1.75}$ or 1.13 (i.e., 13%).

Air sampling rates derived in this study agree with field-derived SPMD values for PCBs (reported mean, 3.6 m^3 d^{-1} for ∑PCB) in the U.K. (*8*). In this study, chambers (Stevenson screens) were used to diminish wind speed effects. Similar values were also reported by Petty et al. (*3*) (approximately 4.7 m^3 d^{-1} for an equivalent SPMD) where mini-SPMDs were deployed in a laboratory and combined as a composite sample.

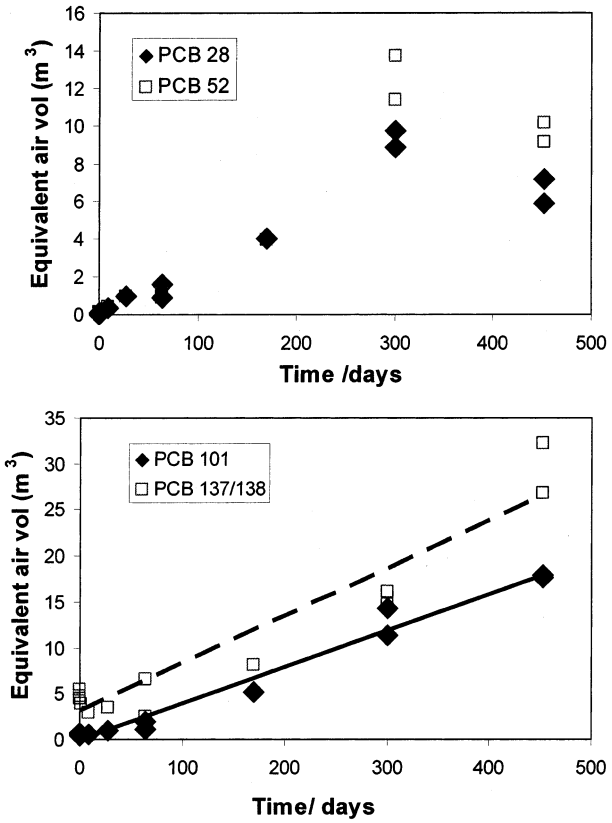

FIGURE 4. Sample profiles for soil for (a) PCBs 28 and 52 and (b) PCBs 101 and 137/138.

When PSM are deployed in outdoor studies, the true sampling rate will depend on the sheltering device used and the orientation of the PSM within the device. Ideally the sheltering device should allow sufficient circulation of air while also providing enough shelter from the wind so that the uptake rate remains fairly uniform and not strongly influenced by differences in wind speeds (e.g., between test sites). Ultimately, the PSM and sheltering device should be tested in controlled wind studies to check this effect.

PUF. The uptake of PCBs 28 and 52 in the PUF disk sampler is shown in Figure 2a and b. Results for PCBs 101 and 137/138 are shown in Figure 3a,b. The uptake behavior is remarkably similar to what was observed for the SPMD. The small difference in uptake rates can be attributed to the 25% larger planar exposure surface area for the SPMD versus the PUF (i.e., 495 and 365 cm^2, respectively) since k_A will be similar for SPMD and PUF. The time to equilibrium is dependent on K_{PSM-A} and the effective thickness of the sampler (eq 4).

Air sampling rates for the PUF disk samplers are shown in Table 3, and in general there is good agreement between PUF disk and SPMD-based sampling rates. Although SPMD rates are slightly greater on a per sampler basis, this difference is resolved when normalized to surface area (Table 3).

Soil. The uptake of PCBs 28, 52, 101, and 137/138 are shown in Figure 4a,b. It appears that for congener 28 (and perhaps 52) the uptake has become curvilinear toward the end of the study. This possibility will be revisited later when times to equilibrium are investigated. The uptake for PCBs101 and 137/138 is linear over the entire duration of the study. Sampling rates on a surface area basis (Table 3) are within a factor of 2 but consistently greater than those for SPMDs and PUF disks. This may be attributed to a gradual increase of the effective soil surface area over the course of the study. As soil was removed from the tray during sampling, the remaining soil flattened out—resulting in a thinner layer and greater surface area per gram of soil. This continued with each consecutive sample. The initial value of 0.5 cm for soil thickness (corresponding to the start of the study) was used in all of the calculations. Because it is an overestimate for the entire study, the resulting sampling rates for soil are also overestimated.

Meijer et al. (*21*, *22*) recently investigated soil−air partitioning of POPs to soil of varying organic contents and validated semiempirical expressions for estimating the soil−air partition coefficient, K_{SA} (i.e., K_{PSM-A} for soil in eq 2):

$$K_{SA} = 0.411\rho_{SOIL}f_{OC}K_{OA} \quad (7)$$

where ρ_{SOIL} is the density of the soil solids, f_{OC} is the fraction organic carbon of soil, and K_{OA} is octanol−air partition coefficient. This expression can be used to calculate K_{SA} for the PCB congeners. The equilibrium (or plateau) concentration can then be estimated by

$$C_{S,EQ} = K_{SA}C_A/\rho_{SOIL} \quad (8)$$

where $C_{S,EQ}$ is concentration in soil at equilibrium and C_A is concentration in air.

The calculation of $C_{S,\,EQ}$ is summarized in Table 4. The results indicate that the amount of PCBs 28 and 52 accumulated in the soil up to day 450 is within a factor of 2 of the estimated equilibrium value. For PCBs 101 and 137/138, the soil has accumulated ~40% and 8% of the equilibrium estimate. As expected, chemicals with higher values of K_{OA} will have large K_{SA} values (i.e., K_{PSM-A}) and take longer to equilibrate according to eq 4. The capacity of the soil (and hence the duration of the linear uptake period) is dependent on the soil organic carbon fraction. The test soil used here had high organic matter content (~10%).

The use of soils as passive air samplers is very promising but not without caveats. Soil uptake will be influenced by soil properties (OC content, density) and meteorological conditions (temperature, humidity). There is also the issue of increased sorptive capacity and holding strength for "aged" soils and very dry soils. All of these factors need to be considered when inferring atmospheric concentrations from soil residue data.

Comparison of MTCs. The uptake of PCBs and PCNs between SPMD, PUF disk, and soil can be compared on a common basis by calculating experimentally derived MTCs or dry deposition velocities (cm s^{-1}). As discussed earlier, this is simply R/A_{PSM} (note that the air sampling rate R is in $cm^3\,s^{-1}$ $sampler^{-1}$). The area for SPMD and PUF disk samplers are 495 and 365 cm^2, respectively. For soil, R is expressed on per gram dry soil basis, so it is necessary to correct by the surface area represented by 1 g of dry soil. This is estimated from the dry soil bulk density (0.71 g cm^{-3}) and the thickness of the exposed soil (0.5 cm) and is equal to 2.82 cm^2 g^{-1} (i.e., $1/(0.5 \times 0.71)$).

Figure 5 compares the calculated air-side MTCs for the three passive sampling media. There is very good agreement, and values are generally in the range of 0.1−0.2 cm s^{-1}. Slightly higher mean values are observed for soil (0.26) as compared to SPMDs (0.13) and PUF disk (0.11). As discussed earlier, the value for soil may be an overestimate related to thinning of the soil layer over the course of the study. These MTCs are very similar to the value of ~0.11 cm s^{-1} used to describe transfer of pesticides across the soil−air interface (*23*). This value is based on a boundary layer thickness of 4.75 mm as derived by Jury et al. (*24*).

Comparison of K_{PSM-A}. By the end of the uptake study (day 450), some of the lower molecular weight compounds were able to establish or nearly establish equilibrium with the sampling media. Results for these compounds can be used to approximate K_{PSM-A}, which is very useful in assessing the uptake rate constant and duration of linear uptake (t_{25})

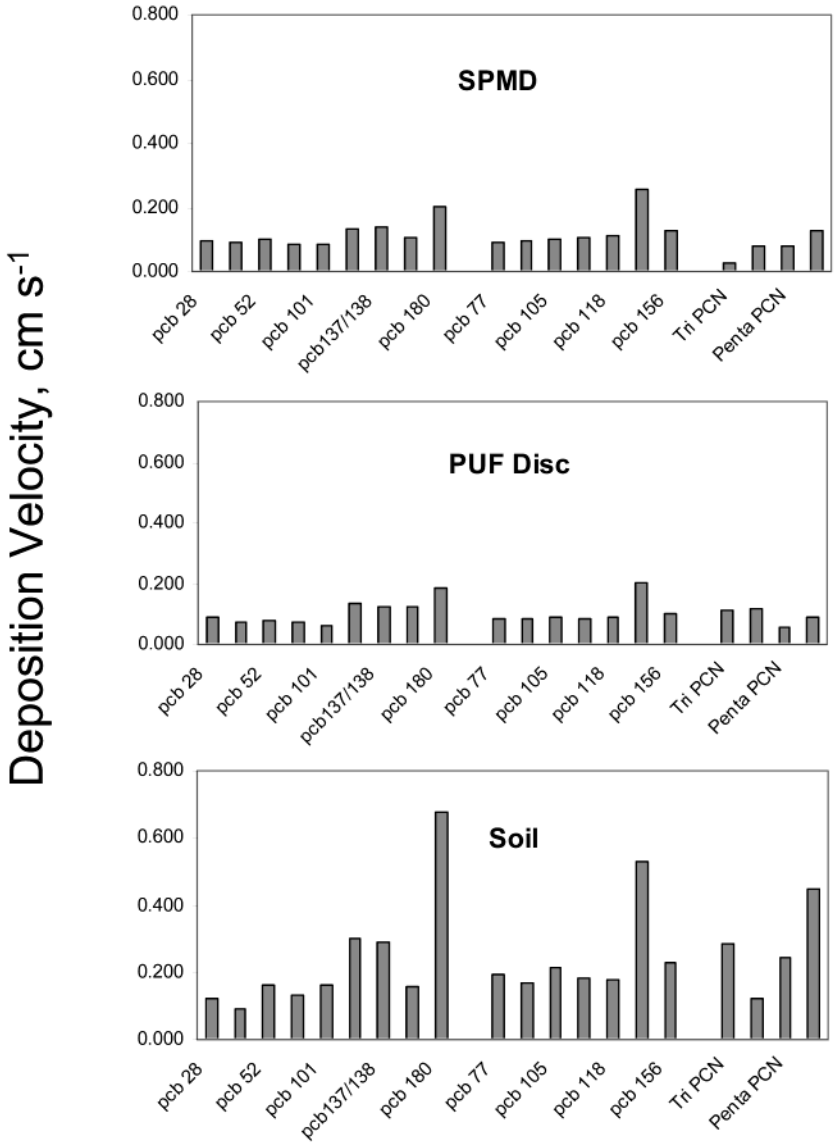

FIGURE 5. Deposition velocities (MTCs, k_A values) for PCBs and PCNs onto SPMD, PUF disk, and soil. MTCs calculated from sampling rates (R', $m^3\ d^{-1}$ sampler^{-1}) as described in Table 3.

and time to equilibrium (t_{95}) using eq 5. Although K_{PSM-A} is defined on a dimensionless basis (see eq 2), it is convenient to also calculate a K'_{PSM-A} on a mass basis (i.e., $K'_{PSM-A} = C_{PSM}$ (ng g^{-1})/C_A (ng m^{-3}) resulting in units of m^3 of air g^{-1}). The two forms of the partition coefficient are related according to $K_{PSM-A} = K'_{PSM-A}\rho_{PSM}$, where ρ_{PSM} is the bulk density of the passive sampler medium in g m^{-3}. Values of C_{PSM}/C_A ($m^3\ g^{-1}$) were calculated in Table 5 for all of the PCBs that were monitored during this study (37 congeners). Average air concentrations for the uptake study and amounts sequestered for each medium at day 450 are listed in the Supporting Information (Supplement 1). Values for day 450 are used because they will be closest to the equilibrium value. Log K_{OA} values at 23 °C (Table 5) were estimated for all PCBs by performing regressions of measured data (*25*) against relative retention times (RRTs) reported by Harju et al. (*26*). More details regarding these calculations are provided in Table 4.

In Figure 6, values of log C_{PSM}/C_A were plotted against log K_{OA} for each medium. On the basis of uptake profiles (Figures 2 and 3, Table 2) congeners 28, 44, and 52 appeared to be at or near the plateau phase by the end of the uptake study. Therefore, for these chemicals C_{PSM}/C_A is equivalent to K'_{PSM-A}. It is also likely that congeners with K_{OA} values lower than PCB 52 (log $K_{OA} = 8.43$) will be at or near equilibrium. Seven congeners met this criteria (18, 17/15, 16/32, 31, 28, 33, and 52) and were used to regress log K_{PSM-A} against log K_{OA}, resulting in the following relationships:

$$\log K_{SPMD-A} = 0.8113 \log K_{OA} - 4.8367 \quad (r^2 = 0.83) \quad \text{(SPMD)} \quad (9a)$$

$$\log K_{PUF-A} = 0.6366 \log K_{OA} - 3.1774 \quad (r^2 = 0.87) \quad \text{(PUF)} \quad (9b)$$

$$\log K_{SOIL-A} = 0.7716 \log K_{OA} - 5.6002 \quad (r^2 = 0.77) \quad \text{(soil)} \quad (9c)$$

The regression equations for eqs 9a and 9c (SPMD and soil) have slopes that are not statistically different than unity ($p < 0.05$). A slope of unity implies that octanol is a good surrogate for the PSM. However, the slope for eq 9b is different than unity ($p < 0.05$). For PUF disk, it may be the case that the higher molecular weight PCBs used to derive the relation to K_{OA} (i.e., PCB 52) have not yet established equilibrium. This would result in lower values of C_{PSM} and explain a slope much lower than unity. For instance when PCB 52 is removed,

TABLE 5. Values of C_{PSM}/C_A at Day 450 and Predicted Values of Log K_{PSM-A} for SPMD, PUF Disks, and Soil Based on Regression Eqs 9a–c[a]

PCB	log K_{OA}	SPMD log(C_{PSM}/C_A)	PUF log(C_{PSM}/C_A)	soil log(C_{PSM}/C_A)	log K'_{SPMD-A}	log K'_{PUF-A}	log K'_{SOIL-A}
18	7.68	1.47	1.75	0.43	1.40	1.71	0.33
17/15	7.70	0.00	1.65	0.35	1.41	1.73	0.34
16/32	7.82	1.43	1.83	0.32	1.51	1.80	0.44
31	8.10	1.65	1.93	0.60	1.74	1.98	0.65
28	8.12	1.88	2.12	0.81	1.75	1.99	0.66
33	8.20	1.73	2.04	0.56	1.82	2.04	0.73
52	8.43	2.05	2.16	0.98	2.00	2.19	0.90
44	8.61	2.01	2.26	0.81	2.15	2.30	1.04
42/37	8.64	2.08	2.41	1.00	2.18	2.32	1.07
74	8.92	2.33	2.38	0.99	2.40	2.50	1.29
70	8.96	2.30	2.34	1.05	2.43	2.53	1.31
95/66	8.99	1.91	2.42	0.93	2.46	2.55	1.34
56/60	9.13	2.43	2.54	1.26	2.57	2.64	1.45
101	9.19	2.51	2.36	1.25	2.62	2.68	1.49
99	9.24	2.43	2.44	1.16	2.66	2.70	1.53
97	9.37	2.40	2.51	1.14	2.77	2.79	1.63
81	9.67	2.32	2.50	1.20	3.01	2.98	1.86
110/77	9.50	2.12	2.52	1.34	2.87	2.87	1.73
151	9.61	2.59	2.53	1.05	2.96	2.94	1.81
149/123	9.71	2.73	2.79	1.52	3.04	3.00	1.89
118	9.96	2.61	2.62	1.52	3.24	3.16	2.08
153	9.91	2.60	2.70	1.21	3.20	3.13	2.05
137/138	10.10	2.70	2.67	1.47	3.36	3.25	2.19
126	10.42	0.00	0.00	0.00	3.62	3.46	2.44
187	10.27	2.80	2.75	1.58	3.50	3.36	2.33
183	10.32	2.86	2.73	1.57	3.53	3.39	2.36
128	10.36	2.69	2.71	1.60	3.57	3.42	2.39
185	10.40	2.96	0.00	1.90	3.60	3.44	2.43
174	10.46	0.00	0.00	0.00	3.65	3.48	2.47
177	10.51	2.95	2.87	1.79	3.69	3.51	2.51
Non-ortho- and Mono-ortho-PCBs							
77	9.75	3.57	3.51	2.43	3.07	3.03	1.92
81	9.67	2.56	2.52	1.24	3.01	2.98	1.86
105	10.17	2.59	2.52	1.51	3.41	3.29	2.24
114	10.04	2.54	2.44	1.35	3.31	3.22	2.15
118	9.96	2.62	2.52	1.39	3.24	3.16	2.08
126	10.42	2.11	1.99	1.04	3.62	3.46	2.44
156	10.75	2.64	2.53	1.52	3.88	3.67	2.69

[a] C_{PSM}/C_A has units of $m^3\ g^{-1}$; C_{PSM} calculated as amount of chemical sequestered by medium divided by its mass in grams (4.41 g for SPMD, 4.40 g for PUF disk, and 1 g for soil). C_A (ng m^{-3}) is the average air concentration listed in Supplement 1 (Supporting Information).

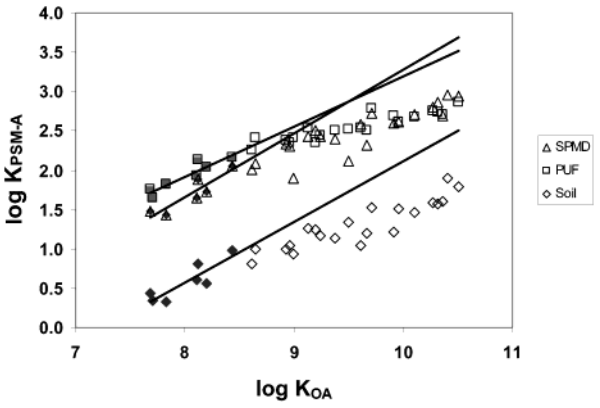

FIGURE 6. Correlation of log(C_{PSM}/C_A) vs log K_{OA} for PCBs for SPMDs, PUF disk, and soil. C_{PSM} is based on amounts sequestered by the sampler up to day 450. Values of C_A and C_{PSM} are presented in Supplement 1 (Supporting Information). (Note: Trend lines are drawn for filled-in symbols representing PCB congeners that have approached equilibrium.) Regression equations are given in the text.

the resulting slope (0.71) is no longer different than unity ($p < 0.05$). It would be useful to confirm these relationships by measuring K_{PSM-A} under controlled laboratory conditions for a larger range of K_{OA} values. In Figure 6, the higher molecular weight PCBs not included in the regression fall below the trend line. This deviation is likely a measure of their departure from equilibrium.

Using the K_{OA}-based expressions for K'_{PSM-A}, values were determined for all the congeners and are listed in Table 5. In Table 6, estimated times to equilibrium (t_{95}) ranged from approximately 2 months for PCB 18 to tens of years for the higher molecular weight 7-Cl PCBs. For a low molecular weight (low K_{OA}) PCB such as congener 18, the time to equilibrium was ~170 days for soil. Congeners 28 and 52 have t_{95} values of ~380 and ~660 days, consistent with Figure 4a that shows a leveling of the uptake curve toward the end of the study. The time required for the soil to become saturated is very dependent on how it was deployed. If deployed in a thinner layer (say 0.1 cm vs 0.5 cm), the time to equilibrium would be five times shorter (~34 days for PCB 18) according to eq 4. Time to equilibrium for PCB 18 in SPMDs and PUF disks was shorter than for soil, occurring near day 50 for SPMDs and later near day 140 for PUF disks. The delay for PUF disks reflects their greater capacity (Z value) for PCB 18 as defined by a larger log K_{PSM-A} value (Table 5)—1.71 for PUF versus 1.40 for SPMD.

The linear uptake region was fairly short for the lower molecular weight PCBs; on the order of one to two weeks for PCB 18 in the three media. When deploying these samplers to estimate air concentrations it is desirable to maintain linear

TABLE 6. Predicted Equilibration Times in Days (using Eqs 4 and 5) for SPMDs, PUF Disks, and 0.5 cm Thick Soil Layer Based on K_{PSM-A} Values in Table 5[a]

	linear phase, t_{25} (day)			equlibrium phase, t_{95} (day)		
PCB	SPMD	PUF	soil	SPMD	PUF	soil
18	5	14	17	50	140	170
17/15	5	15	18	53	150	180
16/32	7	18	23	66	180	230
31	11	26	37	110	260	370
28	11	27	38	110	270	380
33	13	31	44	130	310	440
52	21	43	66	210	430	660
44	29	56	91	290	560	910
42/37	31	58	96	310	580	960
74	52	88	159	520	880	1600
70	55	92	168	550	924	1700
95/66	59	97	179	590	969	1800
56/60	77	120	230	770	1200	2300
101	86	130	256	860	1300	2600
99	93	140	278	930	1400	2800
97	120	170	353	1200	1700	3500
81	210	260	600	2100	2600	6000
110/77	150	210	440	1500	2100	4400
151	190	240	540	1900	2400	5400
149/123	220	280	640	2200	2800	6400
118	360	400	990	3600	4000	9900
153	330	370	910	3300	3700	9100
137/138	470	490	1300	4700	4900	12900
126	850	790	2300	8500	7900	22800
187	640	640	1700	6400	6400	17500
183	700	680	1900	7000	6800	18800
128	750	720	2000	7500	7200	20300
185	820	770	2200	8200	7700	21900
174	910	840	2400	9100	8400	24400
177	990	890	2600	9900	8900	26400
Coplanar PCBs (Analysis by GC−NIMS)						
77	240	290	680	2400	2900	6800
81	210	260	600	2100	2600	6000
105	530	540	1400	5300	5400	14400
114	420	450	1200	4200	4500	11600
118	360	400	990	3600	4000	9900
126	850	790	2300	8500	7900	22800
156	1600	1300	4100	15700	12800	40700

[a] Average MTCs from Figure 6 and effective film thickness of the PSM. Uptake rate constant for each chemical (eq 5) was used to estimate the linear region (t_{25}, time to reach 25% saturation) and time to equilibrium (t_{95}). Mass of samplers are SPMD, 4.41 g; PUF disk, 4.40 g; and soil, 1 g. ρ_{PSM} is the density (g m^{-3}) of the passive sampler medium = 519 000 for SPMD, 21 000 for PUF, and 710 000 for dry bulk soil. The effective film thickness (δ_{FILM}, m) is the volume to surface area ratio. Values used were 0.00017 m (0.17 mm) for SPMD, 0.00567 m (5.6 mm) for PUF disk, and 0.005 m (5 mm) for soil.

uptake for all target chemicals. Thus the values of t_{25} in Table 6 can be used as a guide for setting integration periods for compounds of interest. It is also important to consider that K_{OA} and K_{PSM-A} increase with decreasing temperature. As a rule of thumb (based on the temperature dependence of K_{OA} for PCBs; *25*), K_{PSM-A} will increase by a factor of 2.5−3 for every 10 °C decrease in temperature, resulting in longer linear sampling phases.

Implications. The results from this study confirm that linear uptake by passive air samplers is air-side controlled and therefore mainly dependent upon the surface area and MTC and not necessarily on the type of PSM. For most applications, it is desirable to operate passive air samplers in the linear uptake phase, and so it is important to understand the interelationship between equilibration time, sampler thickness, and K_{PSM-A}. The K_{OA}-based expressions for K_{PSM-A} derived for PCBs in this study for the three sampling media will likely apply to other classes of nonpolar POPs. This can be used to estimate the time to equilibrium that will help to plan and interpret results from passive air sampling studies.

The calibration information presented here is based on deployment in relatively still air (low wind conditions). For outdoor studies, it is necessary that the samplers be deployed in protective chambers that dampen wind speed, which would otherwise result in a reduced boundary layer thickness and variable MTCs. This wind speed effect needs to be assessed for different chamber designs.

Air concentrations can be back-calculated using eq 4 and the average MTCs from Figure 5 and K_{PSM-A} values in Table 5. On the basis of the variability of the calibration data, it is likely that passive sampler-derived air concentrations will provide results that are accurate within a factor of 2 (and perhaps better) of the true values. However, as discussed earlier absolute accuracy may not be essential when a relative comparison is made for passive samplers deployed over the same integration period.

Further research is needed to improve the accuracy and versatility of these devices. Direct measurements of K_{PSM-A} as a function of temperature for SPMDs, PUF disks, and other potential media are required. It is likely that K_{PSM-A} will be well described by K_{OA} as shown here. Another item to address is the degree to which particulate material is sampled by these devices. On this line of thinking, it may be desirable to also develop passive particle samplers since many toxicologically important POPs are strongly associated with particulate matter. Last, it is conceivable that passive sampling will evolve to the stage where samples can be collected with high time resolution, on the order of hours or even minutes. Such an advance would greatly improve our ability to study transport and exchange processes of POPs, which until now have been subject to limitations related to the manner in which active air samplers are collected and analyzed.

Acknowledgments

This work was supported by the Toxic Substances Research Initiative (Project 227), a research program managed jointly by Health Canada and Environment Canada. We also thank Terry Bidleman, Miriam Diamond, and Kevin Jones for their contributions.

Supporting Information Available

Table showing the average air concentrations for PCBs. This material is available free of charge via the Internet at http://pubs.acs.org.

Literature Cited

(1) Llompart, M.; Li, K.; Fingas, M. *J. Chromatogr.* **1998**, *824*, 53−61.
(2) Potter, D. W.; Pawliszyn, J. *Environ. Sci. Technol.* **1994**, *28*, 298−305.
(3) Petty, J. D.; Huckins, J. N.; Zajicek, J. L. *Chemosphere* **1993**, *27*, 1609−1624.
(4) Ockenden, W. A.; Prest, H. F.; Thomas, G. O.; Sweetman, A.; Jones, K. C. *Environ. Sci. Technol.* **1998**, *32*, 1538−1543.
(5) Ockenden, W. A.; Sweetman, A. J.; Prest, H. F.; Steinnes, E.; Jones, K. C. *Environ. Sci. Technol.* **1998**, *32*, 2795−2803.
(6) Huckins, J. N.; Petty, J. D.; Orazio, C. E.; Lebo, J. A.; Clark, R. C.; Gibson, V. L.; Gala, W. R.; Echols, K. R. *Environ. Sci. Technol.* **1999**, *33*, 3918−3923.
(7) Lohmann, R.; Corrigan, B. P.; Howsam, B.; Jones, K. C.; Ockenden, W. A. *Environ. Sci. Technol.* **2001**, *35*, 2576−2582.
(8) Ockenden, W. A.; Corrigan, B. P.; Howsam, M.; Jones, K. C. *Environ. Sci. Technol.* **2001**, *35*, 4536−4543.
(9) Strandberg, B.; Wagman, N.; Bergqvist, P.-A.; Haglund, P.; Rappe, C. *Environ. Sci. Technol.* **1997**, *31*, 2960−2965.
(10) Wilcockson, J. B.; Gobas, F. A. P. C. *Environ. Sci. Technol.* **2001**, *35*, 1425−1431.
(11) Harner, T.; Farrar, N.; Shoeib, M.; Jones, K. C.; Gobas, F. A. P. C. Submitted for publication.

(12) Tremolada, P.; Burnett, V.; Calamari, D.; Jones, K. C. *Environ. Sci. Technol.* **1996**, *30*, 3570−3577.
(13) Calamari, D.; Bacci, E.; Focardi, S.; Gaggi, C.; Morosini, M.; Vighi, M. *Environ. Sci. Technol.* **1991**, *25*, 1489−1495.
(14) Meijer, S. N.; Steinnes, E.; Ockenden, W. A.; Jones, K. C. *Environ. Sci. Technol.* **2002**, *36*, 2146−2153.
(15) Kalantzi, O. I.; Alcock, R. E.; Johnston, P. A.; Santillo, D.; Stringer, R. L.; Thomas, G. O.; Jones, K. C. *Environ. Sci. Technol.* **2001**, *35*, 1013−1018.
(16) Chiou, C. T. *Environ. Sci. Technol.* **1985**, *19*, 57−62.
(17) Harner, T.; Bidleman, T. F. *Atmos. Environ.* **1997**, *31*, 4009−4016.
(18) Harner, T.; Bidleman, T. F. *Environ. Sci. Technol.* **1998**, *32*, 1494−1502.
(19) Whitman, W. G. *Chem. Metal Eng.* **1923**, *29*, 146−150.
(20) Schwarzenbach, R.; Gschwend, P. M.; Imboden D. M. *Environmental Organic Chemistry*; Johns Wiley & Sons Publishers: New York, 1993.
(21) Meijer, S. M.; Shoeib, M.; Jantunen, L. M.; Jones, K. C.; Harner, T. Submitted for publication.
(22) Meijer, S. M.; Shoeib, M.; Jones, K. C.; Harner, T. Submitted for publication.
(23) Harner, T.; Bidleman, T. F.; Jantunen, L. M. M.; Mackay, D. *Environ. Toxicol. Chem.* **2001**, *20*, 1612−1621.
(24) Jury, W. A.; Spencer, W. F.; Farmer, W. J. *J. Environ. Qual.* **1983**, *12*, 558−564.
(25) Harner, T.; Bidleman, T. *J. Chem. Eng. Data* **1996**, *41*, 895−899.
(26) Harju, M. T.; Haglund, P.; Naikwadi, K. P. *Organohalogen Compd.* **1998**, *35*, 111−114.

Received for review March 8, 2002. Revised manuscript received July 17, 2002. Accepted July 24, 2002.

ES020635T